

In this point-to-point answer, please note that the referee's comments are printed in italics, answers to comments are printed in red, while corrections and changes to the manuscript are printed in blue. Changed figures (original figures not included) appear at the end of the document.

The review also gave rise to an improved model setup and the new modelling experiments caused changes off which not all are shown below, but included in the revised manuscript.

Summary:

In this paper, the authors investigate permafrost aggradation and the associated increase in subpermafrost groundwater pressures over millennial scales as the potential cause of pingo springs in a high Arctic valley (Aventdalen, Svalbard). Continuous permafrost, high desert conditions, and a lack of wet-based glaciers in the adjacent highlands preclude recent groundwater recharge as a source of the spring water. Using a 1D heat flow model the authors quantify potential rates of permafrost aggradation. This aggradation is then related to a water flux which is applied as recharge in a 3D groundwater flow model. These processes are fully decoupled. The groundwater flow model represents the steady state flow of groundwater to the pingos (and the adjacent Fjord) that results from the additional subpermafrost water flux. Although validating field data is limited to sporadic spring flow measurements and hydraulic head measurements at a single borehole, what is available is compared to this data to support the development of the model and the proposed conceptualization of the pingo spring flow.

The mechanism proposed by the authors is new, and their use of numerical models to illustrate and quantify this mechanism is of value. The discharge of subpermafrost groundwater to the surface has the potential to introduce methane to the environment and other solutes to freshwater systems. Understanding of the mechanism that generates the driving hydraulic heads in a variety of geological settings improves our ability to forecast future conditions under a changing climate. Overall the conceptual model and the numerical approach is well presented. However, the paper gives the sense that the modelling work proves the conceptual model to be correct. In general, assumptions are made in numerical modelling to align the numerics with the conceptualization. The modelling presented in this paper is no different, and as such, the model output does not prove the conceptual model to be correct. Some factors that warrant further investigation to support the numerical modelling assumptions are detailed below. Value could be added to the paper by using the model to further explore the physical factors required to form pingo springs under this conceptual model.

Freezing pressure from permafrost aggradation is well known from closed-system pingos, but has not previously been considered for open-system pingos as this research does. This is, as also noted by the reviewer, a novelty. Based on our investigation, we argue that permafrost aggradation deserves attention as a driver for deep permafrost springs and open-system pingos. We do so because the modelling results suggest that the conceptual model demonstrates a plausible mechanism for the formation of open-system pingos. However, we do not think that it is the only model for the formation of pingos in Adventdalen, and we try to clarify this in the revised manuscript.

Old version, Abstract, Lines 19:

“Our results show that the pingos in lower Adventdalen easily conform to this conceptual model.”

New version:

“Our results suggest that the conceptual model represents a plausible mechanism for the formation of open-system pingos, and that the pingos in lower Adventdalen conform to this.”

Old version, Sect. 6.3, Line 530:

“The amount of hydrogeological data from Adventdalen was insufficient for automatic calibration of model parameters.”

New version:

“The amount of hydrogeological data from Adventdalen was insufficient for automatic calibration of model parameters and the model simulations should therefore be at best taken as possible scenarios for the conditions in Adventdalen.”

The boundaries of the numerical groundwater flow model create a closed “bathtub-like system. Although the amount of recharge added is quite low (<1 mm/year), the presence of permafrost throughout the top of the model domain, a lower boundary that is within 100 m of the base of the permafrost, and no flow across lateral boundaries, leaves only the Fjord and the pingo springs as discharge points. Additional details, or discussion would be useful in supporting the boundary selection for the groundwater flow model as follows:

1. *The paper investigates the effect of the lower boundary position by lowering the model depth by 100 m. A more illustrative demonstration of the effect of the lower boundary may be to lower the boundary to the detachment zone that separates the upper overpressured and lower underpressured groundwater flow systems (i.e., to a depth where there is field evidence of a no-flow boundary);*

While we agree with the reviewer’s comment that a lower boundary defined by field evidence would be preferred to our somewhat arbitrary approach, there is no such boundary in the investigated system. The reviewer suggests that the detachment zone could define the lower model boundary, but this is found at such shallow depths in the Eastern part of the model area (~ 50 m b.g.l., Fig. 2b) that this would not be part of the groundwater model domain (after the permafrost layer has been removed). Seismic investigations at IHP suggest that pingo spring waters rise vertically from rocks deeper than 50 m (**Rossi et al., 2018**) and thus likely from below the detachment zone. At the same time, hydrogeochemical similarities and consistent trends (water type and concentrations of Cl⁻ and stable water isotopes) from all pingo springs suggest that they formed in the same hydrogeological system (**Hodson et al., In review**). Complete hydrological separation between the lower (NW) and upper (SE) part of the system therefore appears unlikely.

Although no field evidence exists for a uniform model domain depth, it may be justified if we assume that groundwater flow is at least partly controlled by secondary permeability induced by glacial loading and unloading (**Leith et al., 2014b**). We have added this consideration in the discussion of the model extent (see changes in the revised manuscript below the answer to the next comment).

2. *There is no evidence provided for the presence of hydraulic divides at the flanks of the valley that would support the use of lateral no flow boundaries in the groundwater flow model as specified. This boundary prevents any regional flow in to or out of the valley. Were groundwater flow to follow the modest slope of the formations, flux through the Festningen Member may be sufficient*

to dissipate the recharge flux specified in the model. If field data is not available, the sensitivity of model results to deeper regional flow across the valley should be explored;

There is indeed no field evidence for the presence of hydraulic divides at the flanks of valley and we hence write that the lateral model extent is “somewhat arbitrary” (Old version, Section Line 519).

The reviewer suggests that we investigate how regional flow through Festningen member or other presumably permeable hydrogeological units (i.e. fractured bedrock) may affect dissipation of the recharge flux. However, due to its stratigraphical orientation, the Festningen member does not cross the model domain and as such, it cannot facilitate regional flow across the system (Figs. 2b and 4): Eastwards, it is not present, and in the Northeastern part of the domain, it is cut by the surface/Quaternary strata.

Although no field evidence exists for a “bathtub” system, the no flow boundary may be justified as groundwater flow is presumably at least partly controlled by secondary permeability induced by glacial loading and unloading. Modelling experiments of the development of such microcracks below valley landscapes suggest that these are most important below valley bottoms (Leith et al., 2014b, 2014a). This may justify a “bath tub” model domain.

Old version, Section 6.2.2., Lines 518-529:

“Given the lack of known geological boundaries or groundwater divides, the lateral extent of the model domain was defined using a simplified outline of the HML, but this may be somewhat arbitrary. Due to Early Holocene warming (Fig. 3), the 1DHT simulation results showed that continuous frozen ground in Adventdalen is likely younger than 6.5 ka even where the valley floor is older (Fig. 5). This is supported by geomorphological and geochronological evidence (Humlum, 2005). As such, there seems to be no reason why permafrost dynamics outside the HML should be markedly different from that in the up-valley part of the model area. Based on the above, it is possible that basal permafrost aggradation goes on beyond the model area (HML) and model simulations may have underestimated the freezing-induced pressures affecting spring discharge.

The dominantly low-permeable groundwater system challenged a physically determined lower boundary for the model domain. From the significant low-pressures observed in deeper stratigraphic layers (~ 800 m b.g.l., Braathen et al., 2012), we inferred isolation of the investigated groundwater system from that below and simply assigned the base to a depth of 300 m b.g.l. By simulating scenarios with a lower base of 250 and 400 m b.g.l., we found that simulation results did not change significantly (< 1 % deviation of simulated heads and discharge rates).”

New version:

“Despite the relatively extraordinary amount of relevant data available for Adventdalen, the boundary selection still relied on very little information. As such, the boundary conditions are somewhat speculative and at best representative of one possible state of the investigated groundwater system. More data and greater certainty would be preferable, but we are left with this approach in lack of better options. This is a common challenge for modelling deep groundwater flow in permafrost area (van der Ploeg et al., 2012).

The boundary conditions of the groundwater model define a bathtub-like system with the pingo springs and the fjord as the only discharge points. Despite the lack of field evidence from Adventdalen, such as

geological boundaries or groundwater divides, the no-flow boundaries at the valley flanks and the model base may be partly justified if we assume that groundwater flow is at least partly controlled by microcracks induced during glaciation: modelling experiments of the development of microcracks during glacial loading and unloading of valley landscape suggest that these are more extensive below valley bottoms (Leith et al., 2014b, 2014a). As such, alignment of the lateral model extent with the HML may at best be approximate at the valley flanks, but arbitrary at the up-valley end. Due to Early Holocene warming (Fig. 3), the 1DHT simulation results showed that continuous frozen ground in Adventdalen is likely younger than 6.5 ka even where the valley floor is older (Fig. 5). This is supported by geomorphological and geochronological evidence (Humlum, 2005). As such, there seems to be no reason why permafrost dynamics in the valley bottom outside the HML should be markedly different from that in the up-valley part of the model area. Based on the above, it is possible that basal permafrost aggradation goes on beyond the model area (HML) and model simulations may have underestimated the freezing-induced pressures affecting spring discharge.

The predominantly low-permeability groundwater system challenged the use of a physically determined lower boundary for the model domain. However, isolation of the groundwater system in our study from deeper can be inferred on account of the well-known geological conditions and the presence of the significant, low-pressures observed below at ~ 800 m b.g.l. (Braathen et al., 2012). We therefore simply assigned an arbitrary depth of 300 m b.g.l. for the lower boundary and subsequently conducted a sensitivity analysis by simulating scenarios with a lower base of 250 and 400 m b.g.l.. In so doing, we found that results did not change significantly (< 1 % deviation of simulated heads and discharge rates)."

- 3. As stated by the authors, the drain boundaries used to represent the pingo springs are placed within the upper most active cells closest to the spring, but within the Festningen Sandstone. Additional details and discussion of this placement would be of use. Figure 2(a) and Figure 4 indicate that the sandstone is not present at the Innerhytte Pingo. Figure 7 shows that the drain associated with the Førstehytte Pingo is opposite the valley axis from the surface expression. It is understood that the fractured nature of this sandstone could permit the required subhorizontal flow to the pingo; however the paper would benefit from additional discussion of this conceptualization (what is the inferred orientation of the fracturing that allows formation of the pingos). The sensitivity of the model results to the geological unit that the drain boundary is placed in should be discussed;*

The reviewer here points to an error in the unrevised manuscript. The drains representing the pingo springs were placed within the uppermost active cells closest to the spring, but within Festningen Sandstone **if present in the underlying stratigraphy**. As the reviewer rightfully notes, Festningen Sandstone is not present at Innerhytte and River Pingos, and the drains were here placed in the uppermost active cells. The reasoning behind placing the drains within Festningen Sandstone is that the permeability of this unit presumably makes it a pathway for groundwater flow. Assessing the fracture orientation within this unit is beyond the scope of this paper, and its hydraulic conductivity was thus assumed uniform.

Old version, Section 4.3.4., Lines 325-326:

"[...] the drains were assigned to the uppermost active cells located closest to springs, but within the conductive Festningen Sandstone."

New version:

“ [...] the drains were assigned to the uppermost active cells located closest to springs, but within the conductive Festningen Sandstone if present in the underlying stratigraphy (i.e. Lagoon and Førstehytte Pingos, Fig. 4).”

4. *The boundary representing the Fjord is described as being applied to the relevant cells. Please describe this assignment in more detail (are the boundaries assigned to the upper most active layer only, or are they assigned to several layers to the approximate seafloor depth in the Fjord). As the boundary at the Fjord represents the highest flux from the model (approximately 40% to 90% of the total flux) model results can be expected to be very sensitive to the vertical location of this boundary, and should be investigated further; and,*

The reviewer is not sure whether the fjord BC is assigned only to the uppermost active cells only or extended to the approximate depth of the seafloor. Both are true because the fjord depth is less than 5 m. It is not stated in the first submission, but the model extent towards the fjord aligns with the approximate terminus of the tidal flat. We have now drawn the tidal flat on Fig. 2a and made the following correction:

Old version, Section 4.3.1., Lines 276-277:

“The horizontal model boundary was a simplified outline of the valley bottom and the lower boundary was at 300 m b.g.l. (Fig. 4).”

New version

Figure 2

“Towards northwest, the model covers the tidal flat (Fig. 2a), but no other sea-covered areas were included. Elsewhere, the horizontal model boundary was a simplified outline of the HML. The lower boundary was set at 300 m b.g.l. (Fig. 4).”

5. *The potential for subpermafrost discharge to the Adventdalen River has not been considered in the conceptual model development. Rossi et al. (2017) suggest that this discharge may occur near the Innerhytte Pingo. Although the rate of subpermafrost discharge to this River may be low, the potential for it to occur should be considered in the overall balance of flows.*

We are aware of (Rossi et al., 2018) and have now included this reference. The reviewer writes that the potential for subpermafrost discharge to the Adventdalen River has not been considered. Based on seismic surveys (Rossi et al., 2018) suggest the discharge area at Innerhytte Pingo (IHP) may extend some meters below Adventdalen River. In the summer when Adventelva is active, a minor amount of spring discharge directly into the river could very well be overseen, but during winter when the river is dry, all perennial discharge points are easily recognized by continuously growing icings. At IHP, there is only one icing observed (covering the pingo apex and extending down to the river). If the reviewer would like it, we will be happy to include a speculative uncertainty bar on Fig. 8, which could account for the potential minor discharge to the river. However, based on our observations of outflow from the winter icing, this would be less than Liestøl's (1977) estimate of 1 L/s, which is already considered in the balance of flows.

Elsewhere than at IHP, perennial discharge to the river would also result in winter season icings. As these have not been observed, we do not regard discharge of subpermafrost groundwater to the river to be plausible.

No changes to the manuscript were made based on this comment.

In general, further investigation of the effect of these various boundary conditions on the groundwater model results are required before it could be concluded that the model results show that the basal permafrost aggradation produces the hydraulic pressures to sustain the pingo spring water outflows as the authors have stated at the start of Section 7.

The reviewer here refers to the first paragraph of Sect. 7. This paragraph was intended to refer to open-system pingo formation in general, and not specifically to the pingos in Adventdalen. As such, we did not mean to give the impression that the basal permafrost aggradation, per se, produces hydraulic pressures that sustain the outflow in Adventdalen. Instead, we argue that the model experiments show that permafrost aggradation alone may drive open-system pingo and subpermafrost spring systems, if conditions like for the modeling experiments exists.

Old version, Sect. 7, Lines 622-23:

“Results from the decoupled heat and groundwater model show that millennial-scale basal permafrost aggradation may alone produce hydraulic pressures sufficient for the formation of pingos and their spring water outflows.”

New version

“Results from the decoupled heat and groundwater model show that millennial-scale basal permafrost aggradation may alone produce hydraulic pressures sufficient for the formation of pingos and their spring water outflows when the right conditions are met.”

The observed hydraulic head at DH4 is stated to range from 9 m to 60 m above hydrostatic. It is unclear if this range is due to temporal variability, or the range in the correction for the effect of dissolved gasses. With limited field data for model validation, this warrants further discussion. As shown on Figure 7 (2a, 3b, 3a) simulations in which the hydraulic head at DH4 is on the lower end of this range (and with the lower to middle recharge flux) do not produce sufficient flow at the pingo springs.

The range of the “observed” head at DH4 reflects uncertainty. The head range is calculated from a single hydraulic pressure (range) estimate by **(Braathen et al., 2012)** excluding the potential pressure effect of dissolved gasses. This was already stated in the first submission in Sect. 3.1 lines 145-148. **(Braathen et al., 2012)** deduce the plausible hydraulic pressures based on outflow from the well during drilling. We have now expressed this explicitly:

Old version, Line 144:

“Nearby, [...]”

New version:

“Based on artesian outflow during a drilling experiment nearby, ...”

The equivalent recharge applied to the model ranges from 25.4 m³/day to 56.7 m³/day. This range is related to the porosity of the formation through which permafrost aggradation is occurring. Based on the 1D columns shown on Figure 4, and the model results shown on Figure 5, much of this aggradation would occur within the shale units. The porosity of the Janusfjellet subgroup has been derived from Manger (1963). How was the range from 0.1 to 0.3 selected from the values provided in Manger (1963). The higher porosity units in this reference are related to high clay content shales or claystones. Is this valid for the Janusfjellet formation? Given that the higher porosity ranges were required to produce a water flux that could sustain the pingo flows, further details should be provided on the derivation of these values.

Indeed, by being the dominant geological unit, the Janusfjellet Subgroup is where most permafrost aggradation takes place. The porosity values (0.1-0.3) were chosen because Agardhfjellet Formation (Janusfjellet subgroup) is the Svalbard analogue to the Kimmeridge Clay Fm, which in (Manger, 1963) is reported to have porosities between 0.19-0.307 (only two samples from one outcrop location). We realize that basing the most crucial parameter for permafrost aggradation (and thus equivalent recharge) on so little empirical data is insufficient. We have now regarded the estimated burial depths of the Janusfjellet Subgroup (Grundvåg et al., 2019; Marshall et al., 2015) and inferred a porosity range based on empirical works on compressibility of clays and mudstone as function of effective vertical stress (Burland, 1990; Okiongbo, 2011; Yang and Aplin, 2004). Using these new references, we find a possible porosity range of 0.08 to 0.3. See changes to the manuscript below the answer to the comment regarding the hydraulic conductivity range of Carolinefjellet and Helvetiafjellet formations.

How is the lower boundary of the 1D heat transfer model specified? If the geothermal gradient from surface is maintained, does that imply that temperature of the lower boundary changes with time? How would the rate of permafrost aggradation be changed if the depth of the 1D model was extended such that the heat flux at the bottom boundary could be kept constant through time? How would a cessation of permafrost aggradation up valley effect results?

The lower boundary (z=300 m) has a BC defined by a geothermal gradient of 0.025 C/m. Because the geothermal properties in the lowermost cell are constant throughout all simulations (i.e. the pore water does not freeze), this BC is equivalent to a constant heat flux. The reviewer is right that the temperature of the lower boundary changes with time, and we agree that this is problematic. Keeping the remainder of the model setup as before, we have now lowered the lower boundary to a depth of 1 km, so that the temperature change here is close to constant (ΔT less than 0.22, 0.42, and 0.65°C for max, mid, and min porosity scenarios, respectively). The new setup simulates results in different simulated permafrost aggradation rates and we thank the reviewer for helping us improve these estimates.

Old version, Sect. 4.3.3, Lines 311-317:

“The model domain contained 12 one-dimensional grids, each 300 m long and consisting of 150 cells with a height of 2 m. Each individual grid was associated to the model area zones (Fig. 4) and the geothermal properties were defined accordingly. The names of the zones refer to the age of subaerial exposure (Table 1), which defined the simulation run time (e.g. for zone 0-1 the simulation period was 0.5 to 0 ka, for zone 1-2 it was 1.5 to 0 ka, etc. For zone 10, the simulation period was 10 to 0 ka). The initial ground temperature distribution followed the geothermal gradient reported by Liestøl (1977) (0.025 °C m⁻¹) from a surface temperature of 0 °C. At any subsequent time, the lower boundary condition was defined from the same geothermal gradient.”

New version:

“The model domain contained 12 one-dimensional grids, each 1000 m long and consisting of 500 cells with a height of 2 m. Each individual grid was associated to the model area zones (Fig. 4) and the geothermal properties were defined accordingly (deeper than 300 m b.g.l., the properties were that of Janusfjellet Subgroup). The names of the zones refer to the age of subaerial exposure (Table 1), which defined the simulation run time (e.g. for zone 0-1 the simulation period was 0.5 to 0 ka, for zone 1-2 it was 1.5 to 0 ka, etc. For zone 10, the simulation period was 10 to 0 ka). The initial ground temperature distribution followed the geothermal gradient reported by Liestøl (1977) ($0.025\text{ }^{\circ}\text{C m}^{-1}$) from a surface temperature of $0\text{ }^{\circ}\text{C}$. At any subsequent time, the lower boundary condition was defined from the same geothermal gradient resulting a basal temperature change less than 0.65°C .”

In Table 3, the rock unit hydraulic conductivities derived from literature (the Festingen sandstone, the Janusfjellet subgroup, and the detachment zone) range within one order of magnitude across the three scenarios. While this could be considered a large range in this type of study, comparison to the observed hydraulic head at DH4 indicates that Scenario 1 (low hydraulic conductivity) values are unlikely, leaving a more reasonable half order of magnitude range.

We agree with this consideration and narrow the conductivity range of these units in the modeling experiments of the revised manuscript.

Old version, in Table 3:

Festingen Sandstone	Fractured sandstone	10^{-2}	$5 \cdot 10^{-2}$	0.1	0.1
Janusfjellet Subgroup	Shale	10^{-4}	$5 \cdot 10^{-4}$	10^{-3}	0.1
Detachment zone	Fractured shale	10^{-3}	$5 \cdot 10^{-3}$	10^{-2}	0.1

New version, in Table 3:

Festingen Sandstone	Fractured sandstone	$5 \cdot 10^{-2}$	$7.5 \cdot 10^{-2}$	0.1	0.1
Janusfjellet Subgroup	Shale	$5 \cdot 10^{-4}$	$7.5 \cdot 10^{-4}$	10^{-3}	0.1
Detachment zone	Fractured shale	$5 \cdot 10^{-3}$	$7.5 \cdot 10^{-3}$	10^{-2}	0.1

For the rock units with field data (the Carolinefjellet and Hevetiafjellet formations), the hydraulic conductivities applied range over two orders of magnitude. Does this range represent the maximum and minimum of tested values? It would be of value to plot the probability density function for the hydraulic conductivity values for each formation, selecting the geometric mean as scenario 2, and a more realistic percentile as scenarios 1 and 3 to tighten the potential range for these formations. As stated on line 406, the hydraulic conductivity is the most important parameter in determining the distribution of outflows between the pingos and the Fjord. Assignment of this parameter should be constrained where possible.

We agree with the author that the hydraulic conductivity ranges should be tightened where possible. The proposed approach is included in the revised manuscript and the ranges tightened accordingly.

Old version, Section 4.3.2., Lines 290-301

“Due to the sparse data available from the field area, geothermal and hydrogeological properties of the lithologies in the model domain (Tables 2 and 3) were largely based on typical values found in the literature. An exception was the measurements of porosity and vertical permeability, κ_v , in the sandstone units carried out by the Longyearbyen CO₂ Laboratory Project (Olaussen et al., 2020, and references therein). Porosity was found to be the most important parameter for permafrost growth, and realistic minimum, mean, and maximum values were therefore defined for the 1DHT model (Table 2). The small-scale horizontal permeability, κ_h , for sandstones is typically a factor two higher than κ_v (Domenico and Schwartz, 1998). The horizontal hydraulic conductivity, K_h , was therefore calculated using the measurements of κ_v by Braathen et al. (2012) as

$$K_h = C_{Kh/Kv} \cdot \frac{\kappa_v \cdot \rho_w \cdot g}{\mu} \quad (7)$$

where $C_{Kh/Kv}$ is the conversion factor (i.e. 2 for this work), κ_v is permeability [m^2], ρ_w is the density of water [kg m^{-3}], g is the gravitational acceleration [m s^{-2}], and μ is the dynamic viscosity of water [kg (m s)^{-1}]. Ranges of hydraulic conductivity for the fluvio-deltaic succession were based on literature values from (Fitts, 2002). For the bedrock units we also regarded the influence of fractures (Singhal and Gupta, 2010).”

New version

“Due to the sparse data available from the field area, geothermal and hydrogeological properties of lithologies in the model domain (Tables 2 and 3) were largely based on available literature. Porosity was the most important parameter for permafrost growth, and realistic minimum, mean, and maximum values were therefore defined for the 1DHT model (Table 2). The permafrost base is presently located within the upper two thirds of the Janusfjellet Subgroup (Figs. 2b and 4). Estimated burial depths and thicknesses of overlying units (Grundvåg et al., 2019; Marshall et al., 2015) indicate that this strata has been buried to maximum depths between 2150 to 2600 m b.g.l., corresponding to effective vertical stresses between 34 to 41 MPa (assuming a rock density of 2.6 kg m^{-3} and hydrostatic equilibrium). Different studies on the compressibility of lithological and age equivalent rocks in the North Sea suggest porosities between 0.08 and 0.3 (Burland, 1990; Okiongbo, 2011; Skempton, 1969; Yang and Aplin, 2004), so we used this range in our modelling experiments. An exception to the purely literature-based values were the sandstone units, whose matrix porosity and vertical permeability, κ_v , were measured as part of the Longyearbyen CO₂ Laboratory Project (Olaussen et al., 2020, and references therein). The small-scale horizontal permeability, κ_h , for sandstones is typically a factor two higher than κ_v (Domenico and Schwartz, 1998). The horizontal hydraulic conductivity, K_h , was therefore calculated using the measurements of κ_v by Braathen et al. (2012) as

$$K_h = C_{Kh/Kv} \cdot \frac{\kappa_v \cdot \rho_w \cdot g}{\mu} \quad (7)$$

where $C_{Kh/Kv}$ is the conversion factor (i.e. 2 for this work), κ_v is permeability [m^2], ρ_w is the density of water [kg m^{-3}], g is the gravitational acceleration [m s^{-2}], and μ is the dynamic viscosity of water [kg (m s)^{-1}]. The range of the hydraulic conductivity values of the Carolinefjellet and Helvetiafjellet formations (Festningen Sandstone not included) was defined by the 25 %, 50 % and 75 % percentiles of a Weibull probability fit of the measured values (see Supplement). Ranges of hydraulic conductivity for the fluvio-

deltaic succession were based on literature values from (Fitts, 2002). For the remaining bedrock units we also regarded the influence of fractures (Singhal and Gupta, 2010).”

Old version, Sect. 4.3.2., caption to Table 2:

“Density and thermal properties compiled from Bergman et al. (2011) , Williams and Smith (1989), Farouki (1981), and Robertson (1988). Porosities from ^IFitts (2002), ^{II}Braathen et al. (2012), and ^{III}Manger (1963).”

New version, caption to Table 2:

“Density and thermal properties were compiled from Bergman et al. (2011) , Williams and Smith (1989), Farouki (1981), and Robertson (1988). Porosities were from ^IFitts (2002), ^{II}Braathen et al. (2012), and inferred from works by ^{III}Burland (1990), Grundvåg et al. (2019), Marshall et al. (2015), Okiongbo (2011), and Yang and Aplin (2004).”

Old version, Sect. 4.3.2, in Table 2:

Shale 4.73·10⁷ 8002600 0.1^{III} 0.2^{III} 0.3^{III}

New version

Shale 4.73·10⁷ 8002600 0.08^{III} 0.19^{III} 0.3^{III}

Old version, Section 4.3.2., in Table 3:

^ICarolinefjellet Fm Sandstone 10⁻⁴ 10⁻³ 10⁻² 0.1

^Iu. Helvetiafjellet Fm Sandstone 10⁻⁴ 10⁻³ 10⁻² 0.1

New version

^ICarolinefjellet Fm Sandstone 2·10⁻⁴ 5·10⁻⁴ 10⁻³ 0.1

^Iu. Helvetiafjellet Fm Sandstone 2·10⁻⁴ 5·10⁻⁴ 10⁻³ 0.1

In new version of Supplement

“S3 Hydraulic conductivity of Carolinefjellet and Helvetiafjellet Formations

The vertical permeability, κ_v , of the sandstone-dominated Carolinefjellet and Helvetiafjellet formations were measured as part of the Longyearbyen CO₂ Laboratory Project (Olaussen et al., 2020, and references therein). The small-scale horizontal permeability, κ_h , for sandstones is typically a factor two higher than κ_v (Domenico and Schwartz, 1998) and we converted the horizontal hydraulic conductivity, K_h , accordingly (Eq. 7). The ranges of hydraulic conductivity of these units were defined by the 25 %, 50 % and 75 % percentiles of a Weibull probability fit to the measured values (Fig. S5).

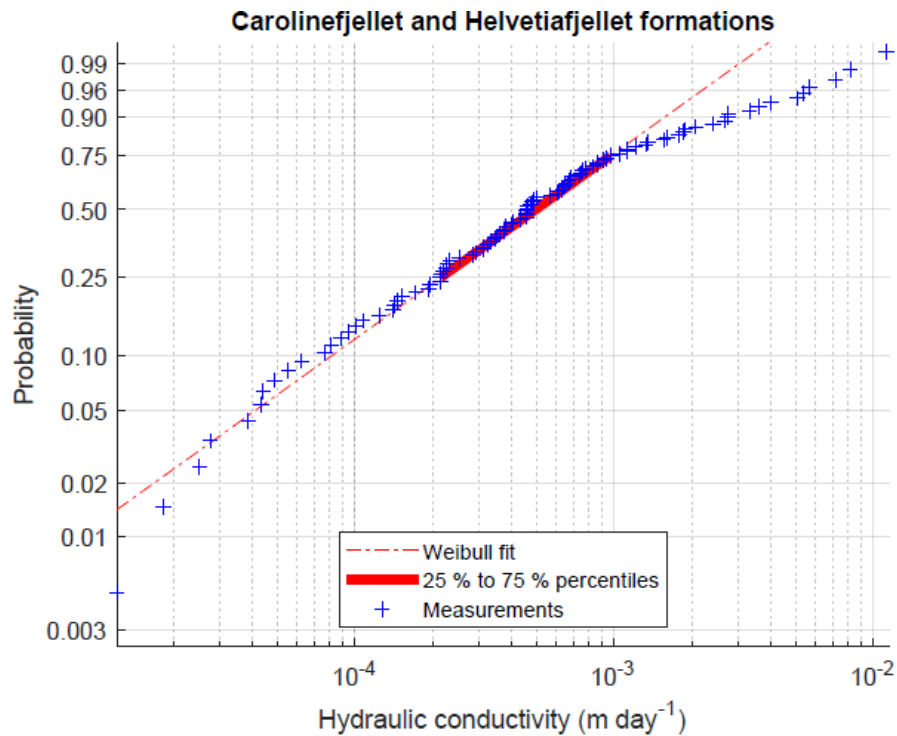


Figure S5 Weibull fit to measured hydraulic conductivities of Carolinefjellet and Helvetiafjellet formations. Original data from the Longyearbyen CO₂ Laboratory Project (Olaussen et al., 2020, and references therein).”

On line 515 it is stated that the steady-state assumption for the groundwater flow model results in an underestimate of the present-day pressures. This statement may oversimplify the transient groundwater dynamics that could occur as permafrost aggrades and the sea level retreats. Permafrost aggradation is highest in proximity to the Fjord, which is also where the greatest potential for discharge to the Fjord occurs. It is possible that any excess pressure would be dissipated as the sea level retreats, and that a transient simulation may not show higher pressures.

As stated in Section 3.2 (lines 182-183), sea-level reached close to present levels ~ 5 ka. As such, the sea retreat since then is due to progradation of the fluvio-deltaic system. Pressure dissipation due to land emergence is therefore not plausible. The statement referred to by the reviewer (Old version, Line 515-516) considers that the omission of dynamic storage effects implies that the predominantly greater permafrost aggradation rates simulated in the past are not taken into account in our model. Effectively, this implies an underestimate of the equivalent recharge. In the revised manuscript, we account for this by applying a moving average to the simulated permafrost aggradation, where the time window is determined by the range of possible adjustment times.

New version, paragraph added to Sect. 4.3.4.:

“The only source of water in the groundwater model was defined from the basal permafrost aggradation rate simulated by the 1DHT model and assigned as recharge to the uppermost active cells in the model domain. To compensate for the lack of dynamic storage effects in the steady-state model, we applied a moving time-average to the simulated basal permafrost growth (or decay) before calculating the recharge equivalent (Eq. 6). The time window of the moving average was based on the possible range of

the adjustment time, t_a , which is the time needed for fluids to redistribute to a pressure perturbation (e.g. Neuzil, 2012; Šuklje, 1969):

$$t_a = l^2 S_s K^{-1} \quad (8)$$

where l is half of the shortest dimension of the system (the characteristic length), S_s is the specific storage, and K is the hydraulic conductivity. We found t_a to be shortest in the vertical dimension, but assumed that hydraulic pressures could only dissipate in the horizontal dimension after the formation of continuous permafrost no earlier than 6 ka (Humlum, 2005; this research). Specifically, we estimated the horizontal t_a to be between 20 and 19000 yrs. To quantify this, we used a characteristic length of 1 km. For S_s , we used a matrix compressibility of $7 \cdot 10^{-10}$ to $7 \cdot 10^{-8} \text{ Pa}^{-1}$ (based on common estimates for fractured rocks, e.g. Domenico and Mifflin, 1965; Domenico and Schwartz, 1998; Fitts, 2002) yielding a S_s of $7 \cdot 10^{-6}$ to $7 \cdot 10^{-4} \text{ m}^{-1}$ (in line with literature values, c.f. Singhal and Gupta, 2010). For K , we used the values estimated for the dominating geological unit (Janusfjellet Subgroup, Table 3). The time window used to compensate for dynamic storage effects were defined from the above, but no longer than the age of permafrost (i.e. 6000 yrs or less)."

On line 635 it was stated that simulated flows to the pingo springs are likely underestimated as basal permafrost aggradation outside of the model domain is not included. Were this aggradation to contribute to the pingo spring flows, it would imply that the lateral boundaries of the model domain are not hydraulic divides (i.e., no flow boundaries). This statement should be reconciled with the boundary selection.

We have not changed the boundary conditions of the groundwater model, but we will be happy to do so if the reviewer also holds the above view for the revised manuscript.

Technical Corrections:

Line 13: ...wet-based glaciers **are not present** in the adjacent highlands

done

Line 18: ...and groundwater (**3D** -Steady-state)

done

Line 229 Equation 1: The $_z$ in the denominator should be $_{zz}$

done

Line 235: ...heat conduction will flow **heat will be conducted** through a matrix of **solids (i.e sediment or rock)** and **liquid water**, ice or a mixture

done

Line 288: ..The fraction of **liquid** water

Done (we assume this correction concerns line 238)

Line 247: ...When temperature change occurs

done

References

Rossi, G., Accaino, F., Boaga, J., Petronio, L., Romeo, R., Wheeler, W., 2018. Seismic survey on an open pingo system in Adventdalen Valley, Spitsbergen, Svalbard. *Near Surface Geophysics* 16, 89–103. <https://doi.org/10.3997/1873-0604.2017037>

References in reply to Reviewer's comments

Bergman, T. L., Lavine, A. S., Incropera, F. P. and Dewitt, D. P.: *Fundamentals of Heat and Mass Transfer*, 7th ed., John Wiley & Sons., 2011.

Braathen, A., Bælum, K., Christiansen, H. H., Dahl, T., Eiken, O., Elvebakk, H., Hansen, F., Hanssen, T. H., Jochmann, M., Johansen, T. A., Johnsen, H., Larsen, L., Lie, T., Mertes, J., Mørk, A., Mørk, M. B., Nemeč, W., Olaussen, S., Oye, V., Rød, K., Titlestad, G. O., Tveranger, J. and Vagle, K.: The Longyearbyen CO₂ Lab of Svalbard, Norway - Initial Assessment of the Geological Conditions for CO₂ Sequestration, *Nor. Geol. Tidsskr.*, 92(4), 353–376, 2012.

Burland, J. B.: *On the compressibility and shear strength of natural clays.*, 1990.

Domenico, P. A. and Mifflin, M. D.: Water from low-permeability sediments and land subsidence, *Water Resour. Res.*, 1(4), 563–576, doi:10.1029/WR001i004p00563, 1965.

Domenico, P. A. and Schwartz, F. W.: *Physical and chemical hydrogeology*, Wiley & Sons., 1998.

Farouki, O. T.: *Thermal Properties of Soils - CRREL Monograph*, US Army Cold Reg. Res. Eng. Lab., 1981.

Fitts, C. R.: *Groundwater Science*, 1st ed., Academic Press., 2002.

Grundvåg, S.-A., Jelby, M. E., Sliwinska, K. K., Nøhr-Hansen, H., Aadland, T., Sandvik, S. E., Tennvassås, I., Engen, T. and Olaussen, S.: Sedimentology and palynology of the Lower Cretaceous succession of central Spitsbergen: integration of subsurface and outcrop data, *Nor. J. Geol.*, 99(2), doi:10.17850/njg006, 2019.

Hodson, A., Nowak, A., Senger, K., Redeker, K. R., Christiansen, H. H., Jessen, S., Hornum, M. T., Betlem, P., Thornton, S., Turchyn, A. V., Olaussen, S. and Marca, A.: Open system pingos as hotspots for sub-permafrost methane emission in Svalbard, *Cryosph. Discuss.*, doi:10.5194/tc-2020-11, 2020.

Humlum, O.: Holocene permafrost aggradation in Svalbard, *Geol. Soc. Spec. Publ.*, 242, 119–130, doi:10.1144/GSL.SP.2005.242.01.11, 2005.

Leith, K., Moore, J. R., Amann, F. and Loew, S.: In situ stress control on microcrack generation and macroscopic extensional fracture in exhuming bedrock, *J. Geophys. Res. Solid Earth*, 119(1), 594–615, doi:10.1002/2012JB009801, 2014a.

Leith, K., Moore, J. R., Amann, F. and Loew, S.: Subglacial extensional fracture development and implications for Alpine Valley evolution, *J. Geophys. Res. Earth Surf.*, 119(1), 62–81, doi:10.1002/2012JF002691, 2014b.

Liestøl, O.: Pingos, springs, and permafrost in Spitsbergen, *Nor. Polarinstitut Årb.* 1975, 7–29, 1977.

Manger, G. E.: Porosity and Bulk Density of Sedimentary Rocks, *Geol. Surv. Bull.*, 1144-E, doi:10.1111/nan.12452, 1963.

Marshall, C., Uguna, J., Large, D. J., Meredith, W., Jochmann, M., Friis, B., Vane, C., Spiro, B. F., Snape, C. E. and Orheim, A.: Geochemistry and petrology of palaeocene coals from Spitzbergen - Part 2: Maturity

- variations and implications for local and regional burial models, *Int. J. Coal Geol.*, 143, 1–10, doi:10.1016/j.coal.2015.03.013, 2015.
- Neuzil, C. E.: Hydromechanical effects of continental glaciation on groundwater systems, *Geofluids*, 12(1), 22–37, doi:10.1111/j.1468-8123.2011.00347.x, 2012.
- Okiongbo, K. S.: Effective Stress-Porosity Relationship above and Within the Oil Window in the North Sea Basin, *Res. J. Appl. Sci. Eng. Technol.*, 3(1), 32–38, 2011.
- Olaussen, S., Senger, K., Braathen, A., Grundvåg, S.-A. and Mørk, A.: You learn as long as you drill; research synthesis from the Longyearbyen CO₂ Laboratory, Svalbard, Norway, *Nor. J. Geol.*, 99(2), 157–187, doi:10.17850/njg008, 2020.
- Robertson, E. C.: Thermal properties of rocks. Report 88-441, US Dep. Inter. Geol. Surv., 106, 1988.
- Rossi, G., Accaino, F., Boaga, J., Petronio, L., Romeo, R. and Wheeler, W.: Seismic survey on an open pingo system in Adventdalen Valley, Spitsbergen, Svalbard, Near Surf. Geophys., 16(1), 89–103, doi:10.3997/1873-0604.2017037, 2018.
- Singhal, B. B. S. and Gupta, R. P.: *Applied Hydrogeology of Fractured Rocks*, 2nd ed., Springer Netherlands., 2010.
- Skempton, A. W.: The consolidation of clays by gravitational compaction, *Q. J. Geol. Soc. London*, 125(1–4), 373–408, doi:10.1144/gsjgs.125.1.0373, 1969.
- Šuklje, L.: *Rheologic Aspects of Soil Mechanics*, 1st ed., Wiley-Interscience., 1969.
- Williams, P. J. and Smith, M. W.: The ground thermal regime, in *The Frozen Earth*, pp. 83–121, Cambridge University Press., 1989.
- Yang, Y. and Aplin, A. C.: Definition and practical application of mudstone porosity-effective stress relationships, *Pet. Geosci.*, 10(2), 153–162, doi:https://doi.org/10.1144/1354-079302-567, 2004.

Changed figures:

Figure 2 – Tidal flat drawn

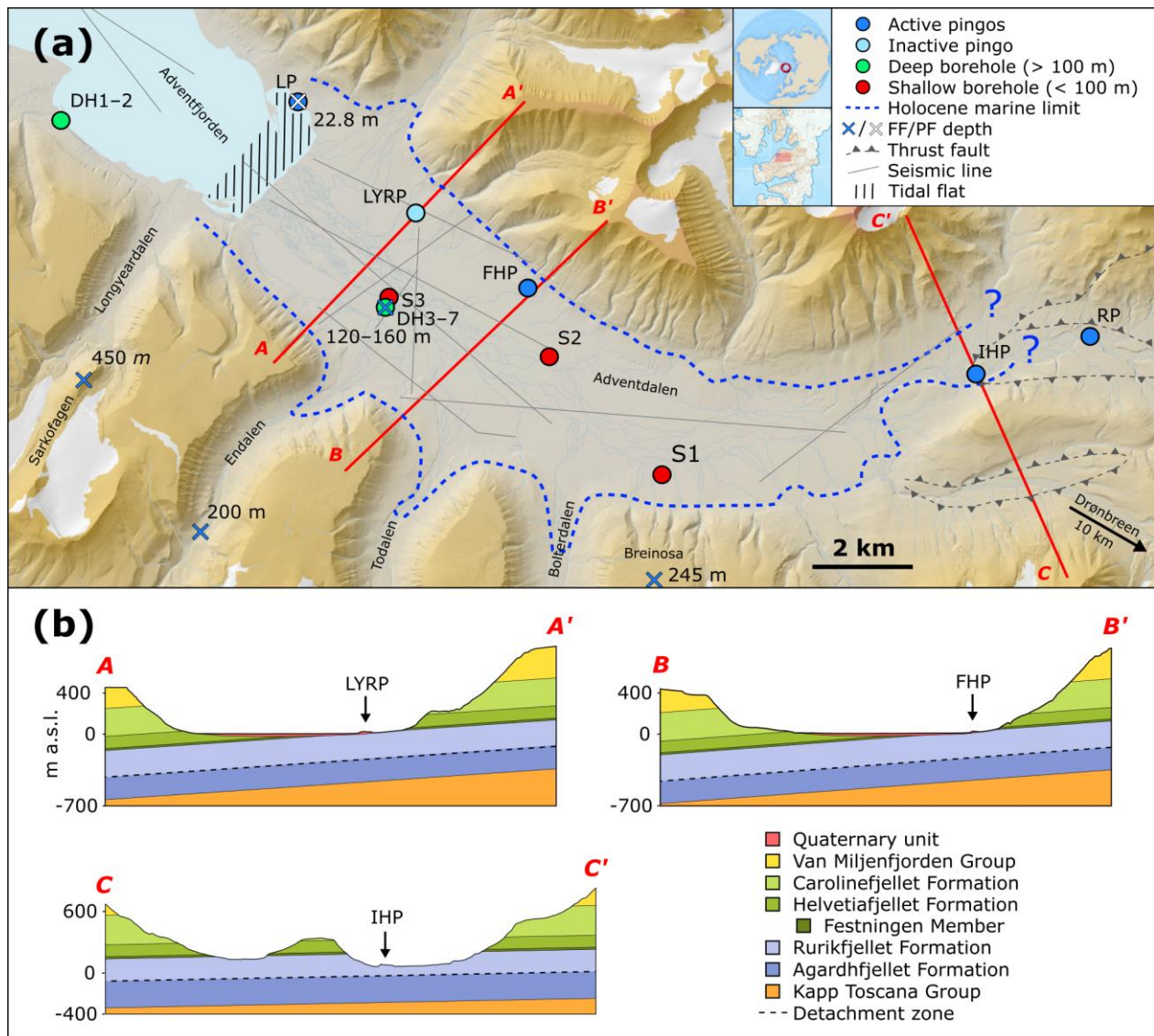


Figure 5 – Changed according to new model setup

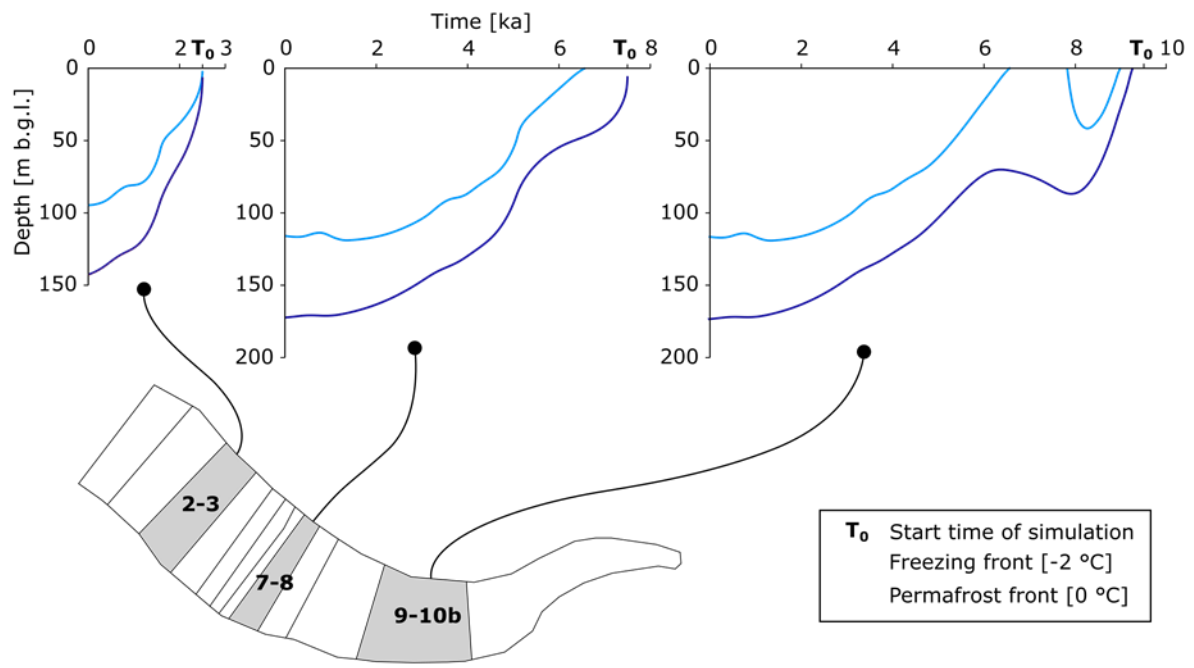


Figure 6 – Changed according to new model setup

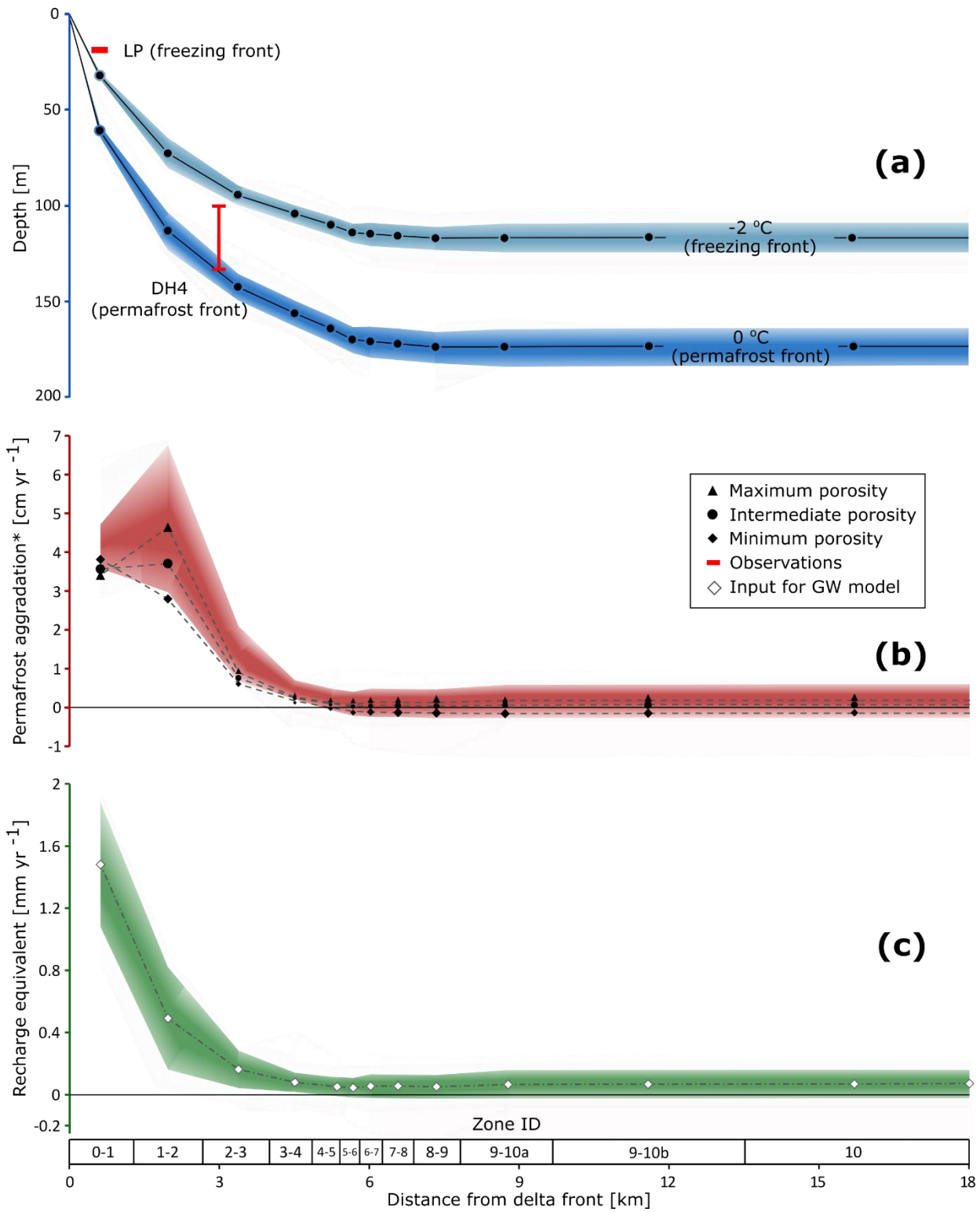


Figure 7 (next page) – Changed according to new model setup

Hydraulic conductivity

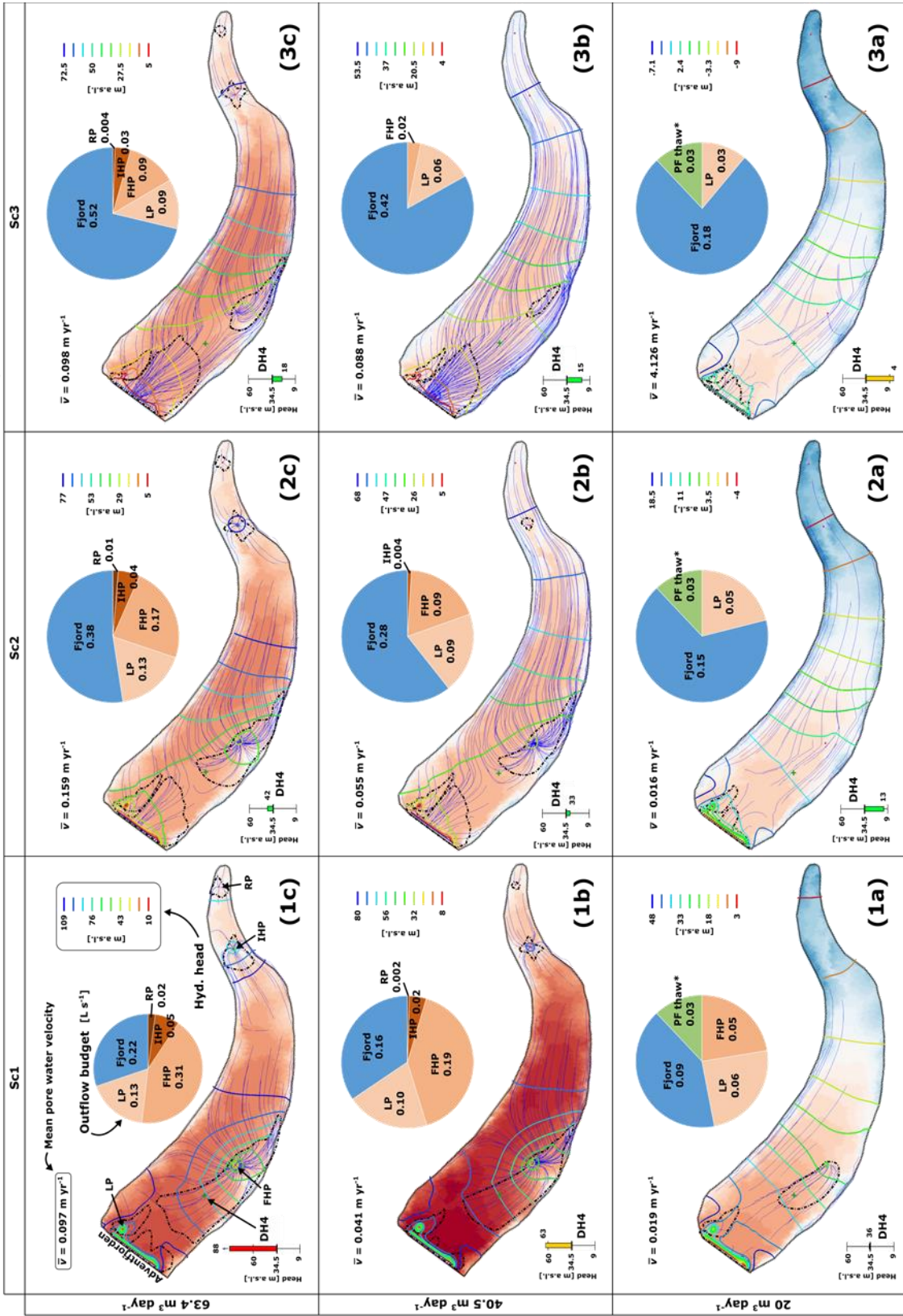


Figure 8 – Changed according to new model setup

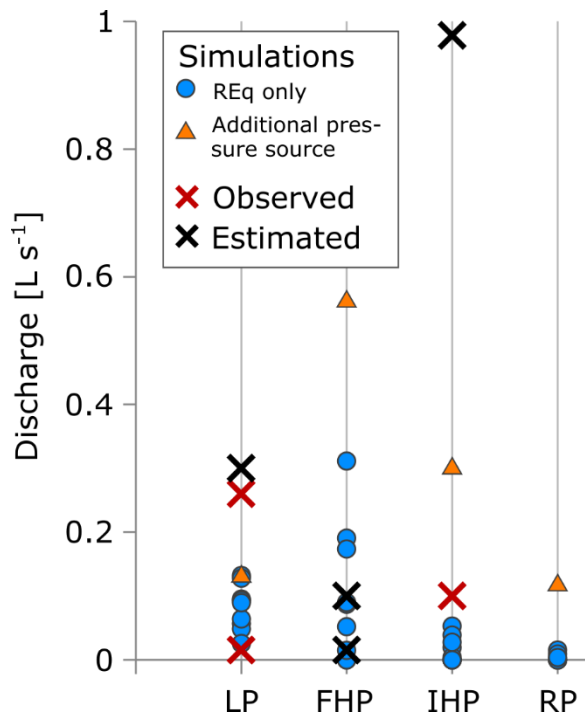


Figure 9 – Changed according to new model setup

